Durability of Surface Mounted PZT and FBG Guided Wave Sensors Under Reusable Launch Vehicle Representative Thermal Cycling

LOIC MASTROMATTEO, LUDOVIC GAVERINA,
JEAN-MICHEL ROCHE, FLORIAN LAVELLE
and FRANCOIS-XAVIER IRISARRI

ABSTRACT

This paper addresses the durability of cobonded PZT and FBG sensors for hybrid Guided Waves (GW) SHM systems under thermal cycles partially representative of a Reusable Launch Vehicle (RLV) use case. The cobonding process is tested as a potential alternative to the secondary bonding process for attachment of SHM sensor network onto composite structures. The evolution of the sensors with the thermal cycles is continuously monitored through measurement of the electromechanical impedance (EMI) spectrums (for PZT) and reflection spectrums (for FBG). Then the effects on the PZT sensors performances are investigated by measuring GW pitch-catch signals at different stages of the thermal cycles. As for FBG sensors, the thermal cycling is still ongoing and is expected to be completed by the time of the conference: additional results will be discussed then.

INTRODUCTION

Over the past decade, the development of reusable launch vehicles (RLVs) to reduce the cost of access to orbit has become a strategic concern for the space industry. However, to achieve this goal, the additional cost of reusability (recuperation and revalidation of stages between launches) must be as low as possible. In this context, SHM systems could help to optimize inspection and maintenance operations on structures. The overall context of this work focuses on the implementation of an hybrid guided waves (GW) SHM system using both PZT transducers for GW sensing and generation and FBG sensors for GW sensing in order to harness the advantages and specificities of both types of sensors. As the SHM sensors networks usually are permanently attached to the structures, the durability of the sensors assembly (sensor+bonding layer) under the environmental and operational conditions is key to the long-term reliability of SHM systems [1]. One of the critical issues for GW sensors is the mechanical coupling between the sensors themselves and the host structure in which GW propagate. PZT transducers are often coupled to the host structure by a secondary

Loïc MASTROMATTEO, ONERA, CNES Paris-Saclay University, 29 Av. de la Division Leclerc, F-92322 Châtillon, FRANCE, Email: loic.mastromatteo@onera.fr

bonding process with an additional adhesive layer. However, the degradation of this adhesive layer can significantly affect the performance of SHM systems, and bonding defects are one of the main durability issues for the sensors. Specifically for composite structures, an alternative to the secondary bonding process is the cobonding process, in which the sensor is applied directly to the uncured composite. The sensor and host structure are then cured together, with the sensor being bonded by the matrix of the composite material. This process, which avoids the use of an additional adhesive layer, could help increase the durability and reliability of the bond between the sensor and the structure. From a manufacturing standpoint, it should also enable a reduction of manual labour required for secondary bonding of large SHM network thanks to the mutualization of the work with the curing of the host structure [2]. This study focuses on testing the cobonding process for PZT and FBG sensors and investigating their durability under thermal cycling. The temperature cycles are chosen to be representative of the thermal loadings that some areas of an actual RLV composite structure under its thermal protection might be subjected to: limited number of cycles (about 10) of short duration (5 minutes) and temperatures up to 150°C. The evolution of the responses of the sensors with the thermal cycling are continuously monitored with a measurement of the electromechanical impedance (EMI) spectrums of the PZT and the reflection spectrums of the FBG. The impact on the GW sensing capabilities is also measured through GW pitch-catch measurements after 0, 5 and 10 thermal cycles. The thermal cycling applied to the FBG sensors has not been completed for the time being; results from these specific tests will be presented at the conference.

METHODOLOGY

Materials and Sensors Layout

The sensors used in this study are C-6 PZT discs from FUJI-Ceramics (20 mm in diameter and 200 µm thick) and 5 mm long uniform FBG from IDIL Fiber Optics. These sensors are attached onto two 350 mm x 400 mm layered T700/M21GC CFRP composite plates, one for each type of sensors (see Figure 1). The quasi-isotropic layout is $[0,-45,90,45]_s$ with a total thickness of 2 mm. The sensors that are submitted to the thermal cycling are arranged in a 30° tilted square to reduce direct wave reflections. All PZT sensors are cobonded to the surface since it was shown in a previous work that

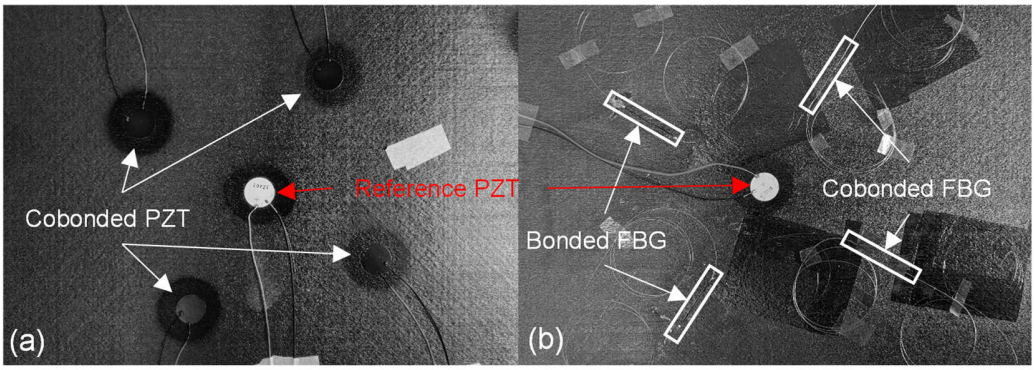

Figure 1: Sensors layout on the composite plate, (a) for the cobonded PZT, (b) for the FBG either bonded or cobonded

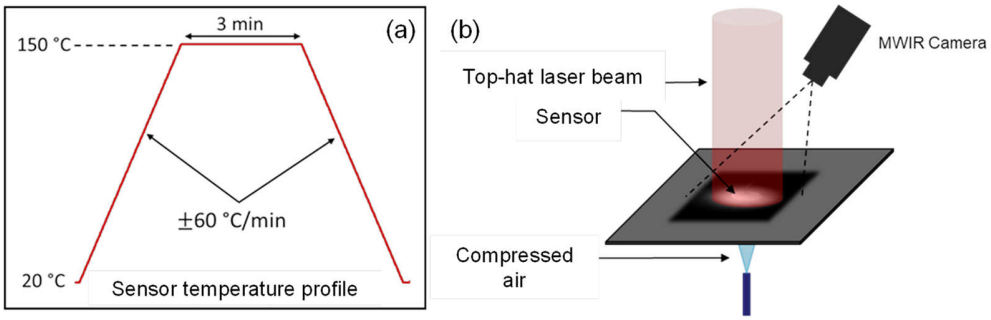

Figure 2: Sensor temperature profile (a) and Laser Thermal cycling setup (b)

cobonding guarantees better durability properties than secondary bonding [3]. As for the FGB sensors, both cobonding and secondary bonding (with a Loctite 495 cyanoacrylate adhesive) are considered in order to evaluate their respective resistance to thermal cycling. In the center of both plates a reference PZT that is not submitted to the thermal cycles is cobonded to emit and receive GW to and from the other sensors.

Thermal cycling setup

The thermal cycle was chosen to be as representative as possible of a thermal environment that RLV composite components might be exposed to during their lifetime (around ten flights of a few minutes each). In contrast to this short exposure time, the thermal loads are intense (high maximum temperatures and steep thermal ramps, as seen in Figure 2) compared to other studies in the literature [4], [5], which often focus on aircraft applications and have much longer and smoother thermal cycles. Ten cycles are applied to the sensors (excepted the central one, used as reference), generated using a CO_2 laser while the backside of the plate is cooled with compressed air in order to reach thermal equilibrium and have stable backside surface temperature during the cycles. The thermal profile at the plate surface is controlled using an MWIR infrared camera. Laser heating has several advantages in our case. First, it allows much steeper thermal ramps than a furnace; second, the generated heating is non-uniform, presenting a thermal gradient between the hot side (where the transducers are located) and the cold side of the coupon. This is typical of the thermal profiles RLV structures are exposed to, as the heat comes from the outside due to the backfiring of the engines while the inside is generally much cooler due to the cryogenic ergols. Finally, the Laser heating makes it possible to apply cycles to one sensor at a time without affecting the others, so the reference transducer remains undamaged.

Sensor characterization

EMI SPECTRUM MONITORING (PZT)

The EMI method is based on the fact that when a PZT is coupled with a host structure, its electrical impedance is related to the mechanical impedance of the structure through the piezoelectric effect that generates a coupling between the mechanical and electrical variables. This method is often used for damage detection [6] but can also be used for the transducers assembly self-diagnosis by identifying the signatures of possible sensor debonding or degradation in the impedance or admittance spectra [7],

[8]. In this study, the electrical admittance spectrums are measured in the [80 - 440] kHz range, using an HP 4194A Impedance Analyzer. This frequency range is chosen to include the main resonance of the PZT transducers and the signature of potential debonding. As the PZT and the host structure form a coupled system, this frequency range of interest strongly depends on the sensors (geometry, piezoelectric and mechanical properties…) and the mechanical properties of the host structure.

REFLECTION SPECTRUM MONITORING (FBG)

In the literature, many approaches have been used for GW sensing with FBG, including different FBG designs or different demodulation technique [9], [10]. In this work we used some widely available uniform FBG sensors and the demodulation for GW sensing is based on the edge filtering technique for its good sensitivity [10]. This technique makes use of the steep edges of the FBG reflection spectrum and a narrow band accordable laser in order to enhance the sensitivity to high frequency but very small strain ultrasonic signals. As this technique depends on the slope of the reflection spectrum, it is relevant to monitor the shape of this spectrum throughout the thermal cycling as possible degradation could impact its shape and thus the slope. The spectrum is monitored using a HBM FS22 FBG interrogator.

GUIDED WAVE PERFORMANCES

The targeted application of this work is for a GW hybrid SHM system coupling FBG for sensing and PZT for sensing and GW generation. Thus, it is interesting to look at the PZT sensor capability to receive and emit GW into the host structure. Due to the presence of a reference, undamaged PZT, it is possible to test the PZT discs both in reception and in emission. As the FBG are passive sensors, they cannot be use to emit GW and thus they are only tested in reception. The GW signals are recorded in the initial state, then after 5 and 10 cycles to evaluate the impact of the thermal cycling. PZT input voltage for the GW generation is a 5-cycle Hanning windowed sinusoidal toneburst at 10 V peak-to-peak. In order to avoid complex mode superposition, the frequency range is limited to have only the two fundamental Lamb wave modes, namely the first antisymmetric (A0) and symmetric (S0) modes. For our composite plate, this limits the frequency at around 350 kHz. Therefore, three measurements are done in the [15-25] kHz range (maximum A0 amplitude) and three in the [150-250] kHz range (maximum S0 amplitude).

RESULTS & DISCUSSIONS

PZT transducers

Concerning the PZT, the results for the cobonded transducers are compared with results from a previous work presented at EWSHM 2022 [3] for secondary bonded PZT. For the evolution of PZT transducers with the thermal cycling, different degradation scenarios were identified in [3], with or without the appearance of PZT debondings. The result for cobonded PZT are compared with the best case scenario in which the bonded PZT do not show any debonding with only an evolution of the adhesive properties. In

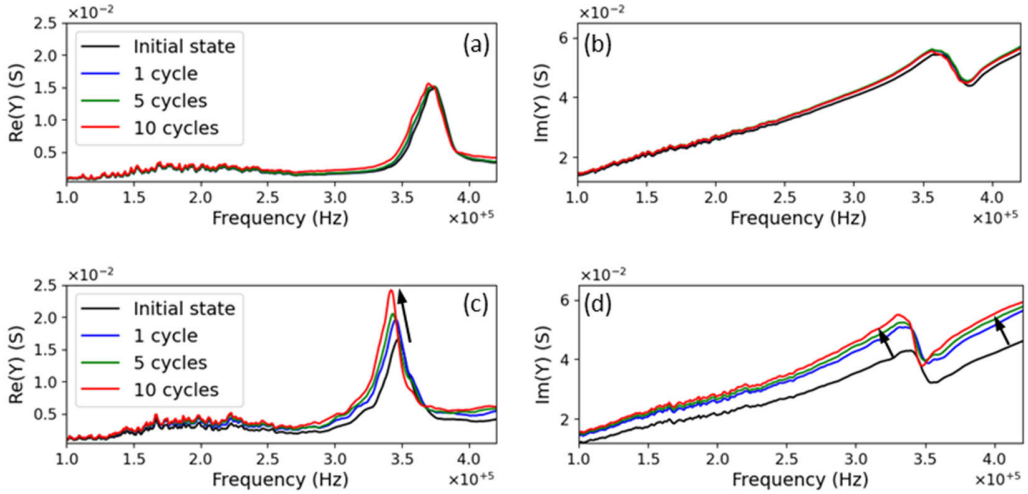

Figure 3: Evolution of the Real and Imaginary part of the admittance for cobonded (a,b) and secondary bonded (c,d) PZT

contrast, for the four cobonded PZT in this work no debonding of the sensors were spotted and every PZT showed a similar behavior throughout the thermal cycling. Figure 3 shows the comparison of the admittance spectrums for one of the cobonded PZT and a secondary bonded PZT (without debonding) [3]. First, we can notice that the evolutions are quite different: for the cobonded PZT disc, the entire spectrum is stable throughout the thermal cycling while for the bonded one a significant evolution of the spectrum can be seen. For the imaginary part, there is an overall increase in the slope of the spectrum. For the real part the impact is the most clear for the resonance peak, with a small downshift in the resonance frequency along with an increase in amplitude. Although a difference can be identified on the admittance spectra, the most important criterion from a SHM standpoint is whether this difference affects the GW performances of the sensors or not. Figure 4 shows the amplitude variation (compared to the initial state) of the GW emitted and received after 5 and 10 thermal cycles for the same PZT discs than in Figure 3. Major differences are spotted regarding the GW performances. On the one hand, cobonded PZT discs present only a few percent variation of amplitude between the initial state and after 10 thermal cycles without a clear visible tendency. On the other hand, the secondary bonded PZT discs are strongly impacted by the thermal cycles, with a 15 % to 20 % drop of amplitude for the reception capabilities. Thus, the

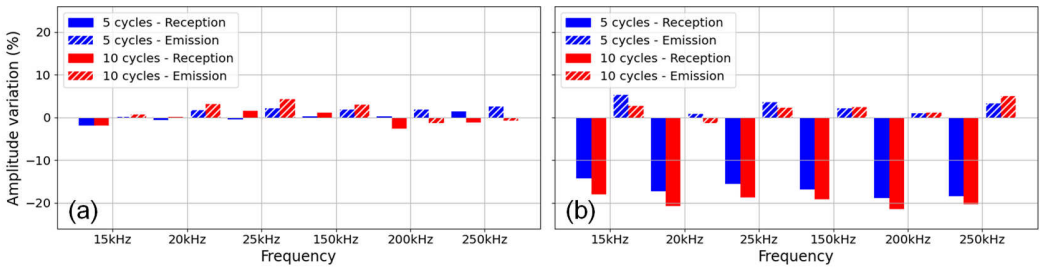

Figure 4: Evolution of the guided wave amplitude with the thermal cycles for a cobonded PZT (a) and a bonded PZT (b)

cobonding process proves to be, in this case, more stable throughout the thermal cycling while also being easier to implement due to the mutualization of the bonding process with the manufacturing of the host structure.

FBG sensors

For the FBG, both cobonded and secondary bonded sensors are tested on the same composite plate with symmetric placement around the reference PZT used to emit the GW. The first important thing to look at is the impact of the bonding process on the reflection spectrum of the FBG. As the edge filtering technique is used to measure the GW signals, the shape of the reflection spectrum and especially its maximum slope will greatly impact the sensitivity of the sensing. The normalized reflection spectrum for one cobonded and one secondary bonded sensors are presented Figure 5 along with the derivative of each spectrum. We can notice that for the secondary bonded FBG the spectrum is only slightly shifted and the shape is almost not impacted with a maximum slope close to the one of the free FBG. For the cobonded FBG the spectrum is much more shifted and its shape is also impacted. This is likely due to residual strain created in the fiber by the shrinkage of the composite matrix during the autoclave curing. We

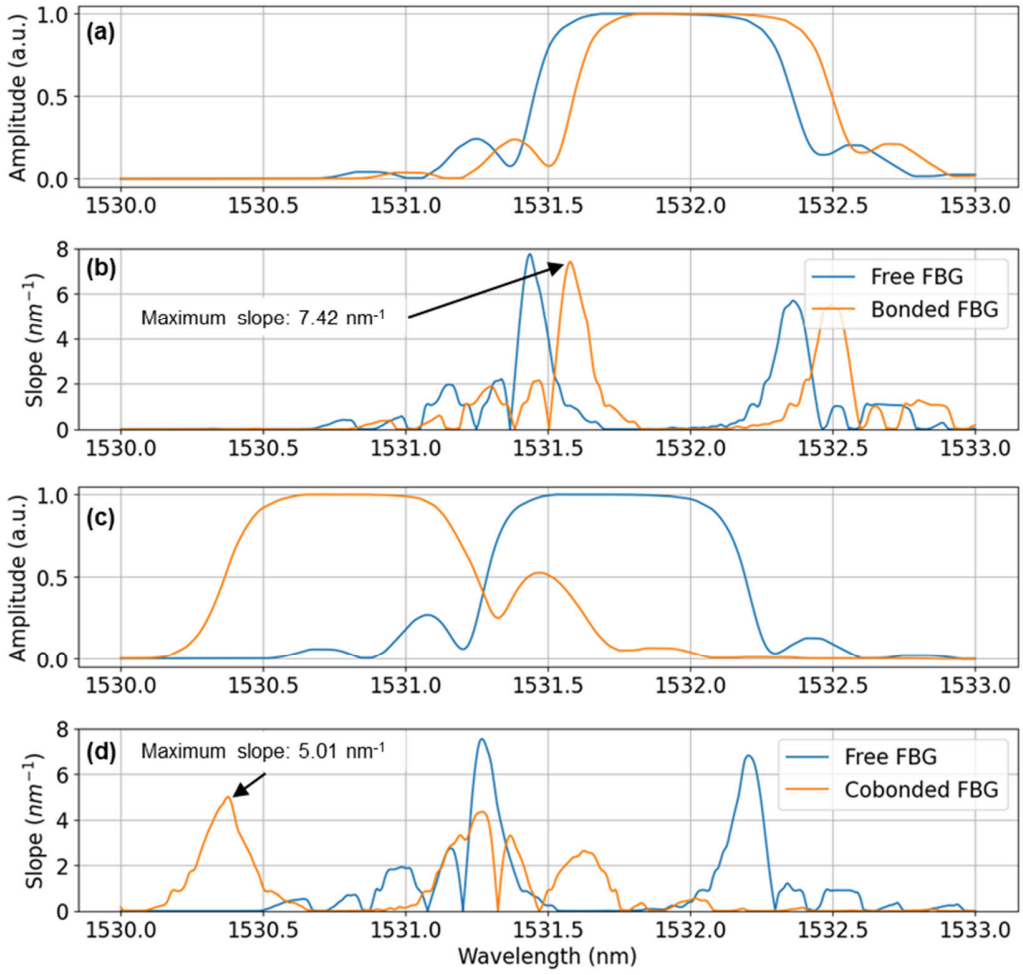

Figure 5: Reflection spectrum and slope for a secondary bonded FBG (a,b) and a cobonded FBG (c,d)

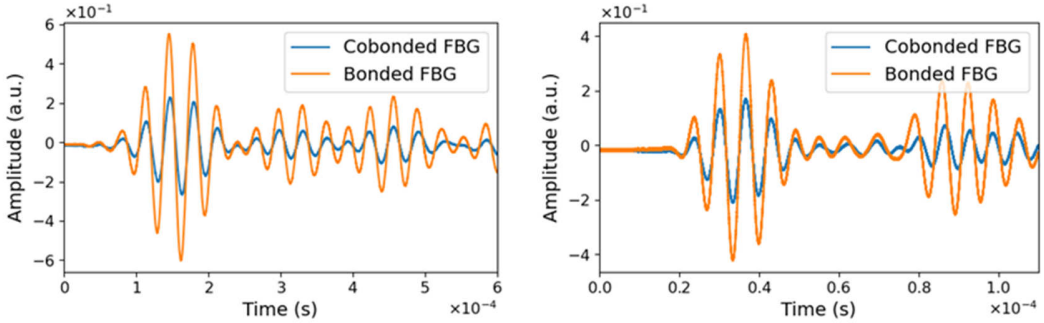

Figure 6: Raw guided wave signals at 30 kHz (a) and 200 kHz (b)

can notice that the maximum slope and thus the optical sensitivity to GW signals is reduced to 5.0 nm^{-1} compared to the 7.4 nm^{-1} for the secondary bonded FBG. However, the slope is only one part of the measurement chain and the strain transfer through the coupling layer plays an important role in the overall measurement of GW signal. Figure 6 shows the baseline raw waveform signal acquired from a cobonded and a secondary bonded FBG placed symmetrically around the reference PZT emitting the GW in the plate. As we can see the amplitude of the raw signals are indeed smaller for the cobonded FBG, nevertheless both signals are in the same order of magnitude and quite similar in the shape of the waveform. This difference of sensitivity should not significantly influence the GW sensing capabilities of the FBG. In fact, for SHM applications, especially when using a baselined approach, the stability of the system throughout the life cycle of the structure will likely be more important for the reliability of the SHM system to avoid false positive and degraded detection capabilities.

Given the previous results for the cobonded PZT transducers showing a good stability throughout the thermal cycles the same kind of behavior is expected for the cobonded FBG compared to the secondary bonded ones.

CONCLUSIONS AND PERSPECTIVES

In this paper, the potential of the cobonding process to attach SHM PZT and FBG sensors to RLV composite structures was tested in comparison with the classic secondary bonding process.

First, from a manufacturing standpoint, the cobonding process was proven faster and produced a more controlled and reproducible bonding than the secondary bonding process thanks to less manufacturing steps and a better control over the bonding process as it is paired with the curing process of the host structure.

Second, regarding the durability stake, the cobonded PZT sensors submitted to thermal cycling did not show any significant evolution or negative impact on their performances. This is in stark contrast with the results obtained for secondary bonded PZT in a previous work [3] in which significant impacts were observed due to debondings and evolution of the adhesive layer properties. Although work could be done to optimize the secondary bonding process for a specific use case (more suitable adhesive, surface preparation), the cobonding process showed a better durability and

reproducibility of the bonding with a simpler and easily implemented process as most of the work is already done for the manufacturing of the host structure.

Lastly, the cobonding process seems to be also suitable for FBG sensors as cobonded FBG were perfectly functional, although with a slightly reduced sensitivity compared to the ones attached to the plate by secondary bonding. A distortion of the FBG spectrum during the curing in autoclave might be responsible for this. The durability to the thermal cycling was not completed in time to be included in this article, but given the good stability observed for cobonded PZT, promising results for the cobonded FBG are expected as well. These upcoming results will be presented and discussed during the conference.

REFERENCES

1. R. Gorgin, Y. Luo, and Z. Wu, 'Environmental and operational conditions effects on Lamb wave based structural health monitoring systems: A review', *Ultrasonics*, vol. 105, p. 106114, Jul. 2020, doi: 10.1016/j.ultras.2020.106114.
2. N. Dobmann, M. Bach, and B. Ekcstein, 'Challenges of an Industrialized Acousto-Ultrasonic Sensor System Installation on Primary Aircraft Structure', presented at the EWSHM 2014, Nantes, 2014.
3. L. Mastromatteo, L. Gaverina, F. Lavelle, J.-M. Roche, and F.-X. Irisarri, 'Thermal Cycling Durability of Bonded PZT Transducers Used for the SHM of Reusable Launch Vehicles', in *European Workshop on Structural Health Monitoring*, P. Rizzo and A. Milazzo, Eds., in Lecture Notes in Civil Engineering, vol. 254. Cham: Springer International Publishing, 2023, pp. 727–736. doi: 10.1007/978-3-031-07258-1_73.
4. M. Salmanpour, Z. Sharif Khodaei, and M. Aliabadi, 'Airborne Transducer Integrity under Operational Environment for Structural Health Monitoring', *Sensors*, vol. 16, no. 12, p. 2110, Dec. 2016, doi: 10.3390/s16122110.
5. V. A. Attarian, F. B. Cegla, and P. Cawley, 'Long-term stability of guided wave structural health monitoring using distributed adhesively bonded piezoelectric transducers', *Structural Health Monitoring*, vol. 13, no. 3, pp. 265–280, May 2014, doi: 10.1177/1475921714522842.
6. W. Na and J. Baek, 'A Review of the Piezoelectric Electromechanical Impedance Based Structural Health Monitoring Technique for Engineering Structures', *Sensors*, vol. 18, no. 5, p. 1307, Apr. 2018, doi: 10.3390/s18051307.
7. S. Park, G. Park, C.-B. Yun, and C. R. Farrar, 'Sensor Self-diagnosis Using a Modified Impedance Model for Active Sensing-based Structural Health Monitoring', *Structural Health Monitoring*, vol. 8, no. 1, pp. 71–82, Jan. 2009, doi: 10.1177/1475921708094792.
8. X. Jiang, X. Zhang, T. Tang, and Y. Zhang, 'Electromechanical impedance based self-diagnosis of piezoelectric smart structure using principal component analysis and LibSVM', *Sci Rep*, vol. 11, no. 1, p. 11345, Dec. 2021, doi: 10.1038/s41598-021-90567-y.
9. R. Soman, J. Wee, and K. Peters, 'Optical Fiber Sensors for Ultrasonic Structural Health Monitoring: A Review', *Sensors*, vol. 21, no. 21, p. 7345, Nov. 2021, doi: 10.3390/s21217345.
10. Q. Wu, Y. Okabe, and F. Yu, 'Ultrasonic Structural Health Monitoring Using Fiber Bragg Grating', *Sensors*, vol. 18, no. 10, p. 3395, Oct. 2018, doi: 10.3390/s18103395.